Aqueous Laponite Clay Dispersions in the Presence of Poly(ethylene oxide) or Poly(propylene oxide) Oligomers and their Triblock Copolymers

R. De Lisi,[†] M. Gradzielski,[‡] G. Lazzara,[*,†] S. Milioto,[†] N. Muratore,[†] and S. Prévost[‡,§]

Dipartimento di Chimica Fisica "F. Accascina", Università degli Studi di Palermo, Viale delle Scienze, Parco D'Orleans II, 90128 Palermo, Italy, Stranski Laboratorium für Physikalische and Theoretische Chemie, Institut für Chemie, Technische Universität Berlin, Strasse des 17. Juni 124, 10623 Berlin, Germany, and Hahn-Meitner Institut (HMI), Berlin, Glienicker Strasse 100, 14109 Berlin, Germany

Received: March 19, 2008; Revised Manuscript Received: May 6, 2008

The effect of polyethylene oxide (PEO) or polypropylene oxide (PPO) oligomers of various molecular weight (M_w) as well as of triblock copolymers, based on PEO and PPO blocks, on aqueous laponite RD suspensions was studied with small-angle neutron scattering (SANS). The radius of gyration (R_G) increases for low M_w whereas the opposite occurs for larger M_w. This behavior is explained on the basis that an effective R_G is given by two contributions: (1) the size of the particles coated with the polymer and (2) the interactions between the laponite RD particles which are attractive for small and repulsive for large polymers. The SANS curves in the whole Q-range are well described by a model of noninteracting polydisperse core + shell disks, where the thickness of the polymer layer increases with the M_w. The adsorbed polymer is in a more compact conformation compared to a random coil distribution while the fraction of the polymer in the shell formed around the laponite RD particles is nearly independent of M_w. For increasing laponite RD amounts, at a given polymer composition, the thickness of the polymer slightly changes. In some cases, where also gelation is sped up, a structure factor with attractive interaction was employed which allowed to evaluate the attractive forces between the laponite RD particles. The gelation time was determined for mixtures at fixed copolymer and laponite RD concentrations. Surprisingly, it is observed that gels are formed despite the fact that the binding sites of the laponite RD particles are almost covered but the polymer size is too small to prevent aggregation. The gelation rate is correlated to structure and thermodynamics of these systems. Namely, when the balance between the steric forces and the depletion attractive forces undergoes an abrupt change the gelation time also undergoes a sharp variation. For lower and comparable M_w, PPO speeds up the gelation more efficiently than PEO while for higher M_w the gelation kinetics is slowed down again. Interestingly, copolymers of PEO and PPO blocks do not induce gelation in the time-window where the homopolymers do.

Introduction

Millions of tons of clay minerals (kaolinite, smectite, sepiolite, etc.) are used annually in a large variety of applications because they are abundant over the world and their cost is very low. However for more advanced applications, synthetic clays[1,2] are often preferred due to their well-established structure, large surface area and higher purity. Laponite RD clay is an example and like other clay particles[3,4] its aqueous suspensions undergo a sol−gel transition above a certain concentration.[5–7]

Polymers are added to the laponite RD suspensions because they modify the rheological properties, are stabilizers or may form new materials like nanocomposites.[8–10] Small angle neutron scattering (SANS)[11] and dynamic[12] and static[13] light scattering techniques as well as calorimetry[14] evidenced that poly(ethylene oxide) (PEO) and poly(propylene oxide) (PPO) adsorb on the laponite RD surface. Dynamic light scattering studies evidenced the adsorption of PEO on colloidal silica particles.[15]

SANS[12] and thermodynamic[14] experiments showed that triblock copolymers based on PEO and PPO are more effective than the corresponding homopolymers in building up a steric barrier around the laponite RD particle. As concerns the laponite RD gel formation, in spite of the number of publications, the mechanism of action of the polymer is still not fully understood. Rheological studies[16–20] have shown that PEO of high molecular weight (M_w) retard the aggregation and the gelation of laponite RD suspensions. It was recently reported[21] that the addition of PEO with M_w ranging between 13×10^3 and 60×10^3 g mol^{-1} melts the laponite RD glass while PEO with larger M_w causes re-entrance into a solid soft structure. However, to the best of our knowledge, no information on the effect of short PEO and PPO oligomers on laponite RD gelation is available. Therefore our study discusses in a comprehensive way this aspect to extend these investigations for a more complete range of molecular weights. For the structural investigation SANS experiments were performed and the gelation time in the absence and the presence of shear was determined for laponite RD dispersed in the aqueous mixtures of PEO and PPO with M_w ranging between 200 and 35000 g mol^{-1}. To compliment this study also their monomers were studied. Finally, triblock copolymers, based on PEO and PPO blocks (Pluronics), were investigated in order to elucidate the role of the flanking by the different blocks and having the additional factor of amphiphilicity incorporated into the adsorbing polymers.

* Corresponding author. E-mail: g.lazzara@unipa.it. Telephone: +39 091 6459834. Fax: +39 091 590015.

† Dipartimento di Chimica Fisica "F. Accascina", Università degli Studi di Palermo.

‡ Stranski Laboratorium für Physikalische and Theoretische Chemie, Institut für Chemie, Technische Universität Berlin.

§ Hahn-Meitner Institut (HMI), Berlin.

10.1021/jp8024073 CCC: $40.75
Published on Web 07/12/2008

TABLE 1: Structures and Abbreviations for Block Copolymers Used in This Study

structure	abbreviation	EO/PO (g/g)	M_w (g/mol)
$EO_{13}PO_{30}EO_{13}$	L64	0.66	2900
$EO_{76}PO_{29}EO_{76}$	F68	4.0	8400
$EO_{103}PO_{39}EO_{103}$	F88	4.0	11400
$EO_{132}PO_{50}EO_{132}$	F108	4.0	14600
$EO_{11}PO_{16}EO_{11}$	L35	1.0	1900
$PO_8EO_{23}PO_8$	10R5	1.1	1950

Materials and Methods

Chemicals. Laponite RD grade was a gift from Rockwood Additives Ltd. 1,2-ethanediol (EG) and poly(ethylene oxide) (200, 400, 900, 1500, 2000, 4600, 20000 and 35000 g mol^{-1}), 1,2-propanediol and poly(propylene oxide) (425 and 725 g mol^{-1}) are Fluka products. As block copolymers (BASF products) are (ethylene oxide)$_a$−(propylene oxide)$_b$−(ethylene oxide)$_a$ ($EO_aPO_bEO_a$) where a and b indicate the repetitive number of EO and PO units, respectively. They are summarized in Table 1. D_2O (99.9% isotopic purity) was purchased from Eurisotop. All chemicals were used as received. Water from reverse osmosis (Elga model Option 3) having specific resistivity higher than 1 MΩ cm was used. The procedure to prepare the laponite RD dispersion has been described elsewhere.[14]

Small Angle Neutron Scattering. The small-angle neutron scattering (SANS) experiments were performed at the Hahn-Meitner Institute, Berlin, Germany, on the instrument V4.[22] A wavelength of 6.0 Å was selected. The sample to detector distances of 1, 4, and 12 m were employed in order to cover the Q-range of 0.03 − 4 nm^{-1}. The data were registered on a 64 × 64 two-dimensional detector, afterward radially averaged and converted into absolute units, i.e., the differential cross-section $I(Q)$, by comparison with the scattering of an 1 mm H_2O sample and proper correction for detector background and the scattering of the empty cell.[23,24] The data treatment was done by the standard software BerSANS.[25] However, it should be noted that the incoherent scattering was not subtracted from the intensity curves shown in the following. The SANS experiments were carried out at fixed polymer composition (1 wt %) and employing laponite RD concentrations of 0.5 and 1 wt %, which do not form gels in at least 1 month. Two different contrasts were employed by changing the solvent: D_2O and a mixture of D_2O + H_2O (31.5% H_2O) which matches laponite RD.[11]

SANS Data Analysis. The data at low value of the scattering vector (Q) were analyzed by means of the Guinier approximation according to eq 1

$$\ln[I(Q)] = \ln[I(Q=0)] - R_G^2Q^2/3 \quad (1)$$

where R_G is the radius of gyration of the scattering particle. Even for the case that interactions are not negligible, eq 1 is still valid but then R_G assumes a more general meaning of a characteristic length of the system plus an interaction parameter that arises from the structure factor.[26] This means that this procedure always allows to extrapolate correctly to the zero-angle scattering intensity $I(Q = 0)$, provided that the system is composed of individual particles and has no longer length scale than covered by the scattering experiment.

For all of the systems exhibiting a plateau of the scattering intensity at low Q, the scattering function could be well described by a model of noninteracting core + shell disk with polydisperse radius. On the basis of this model, the scattering intensity is given by[11]

$$I(Q)_{disk} = {}^1N_{disk}P(Q, R, \sigma_R, h, \Delta R, \rho_{RD}, \rho_{solvent}, \rho_{shell}) \quad (2)$$

where ${}^1N_{disk}$ is the number density of disks and $P(Q, R, \sigma_R, h, \Delta R, \rho_{RD}, \rho_{solvent}, \rho_{shell})$ is the core + shell disk form factor[11] given by

$$P(Q) = \int_0^{\pi/2} \sin\theta\, d\theta \left[V_{shell}(\rho_{shell} - \rho_{solvent}) \times \frac{\sin[Q(h+2\Delta R)(\cos\theta)/2]}{Q(h+2\Delta R)(\cos\theta)/2} \frac{2J_1[Q(R+\Delta R)\sin\theta]}{Q(R+\Delta R)\sin\theta} + V_{RD}(\rho_{RD} - \rho_{shell}) \frac{\sin[Qh(\cos\theta)/2]}{Qh(\cos\theta)/2} \frac{2J_1[QR\sin\theta]}{QR\sin\theta} \right]^2 \quad (3)$$

where R is the radius and h the thickness of the disk while ΔR is the polymer adsorbed thickness assumed to be equal at both the face and the edge; σ_R is the mean standard deviation for the particle radius obtained considering a normalized zeroth order logarithmic distribution.[11] ρ_{RD}, $\rho_{solvent}$, and ρ_{shell} are the scattering length densities of laponite RD, solvent and shell, respectively. V_{shell} and V_{RD} are the volume of the shell and the core, respectively. J_1 is the first-order Bessel function and θ is the angle between the normal to the face and the scattering vector Q.

For the data of the pure laponite RD dispersed in D_2O, ΔR was of course set equal to zero, R, σ_R, and h were determined from the best fit by fixing the contrast ($\rho_{solvent} = \rho_{D_2O} = 6.37 \times 10^{10}$ cm^{-2} and $\rho_{RD} = 4.18 \times 10^{10}$ cm^{-2})[11] and the number density of particles calculated as $\phi_{RD}/\pi R^2 h$ where ϕ_{RD} is the volume fraction of laponite RD.

As concerns the laponite RD + polymer + solvent mixtures, in a first step of the analysis the polymer was assumed to be all in the adsorbed state but poor fits were obtained. The thermodynamics[14] of adsorption of polymers on the laponite RD particles indicates that some amount of polymer is freely dispersed in the solvent and therefore its contribution to the total scattering intensity was taken into account by means of the Debye equation[27] for a noninteracting random coil

$$I(Q)_{chain} = \frac{c_p x_p M_w}{N_{Av} d_p^2} (\rho_p - \rho_{solvent})^2 \frac{2}{x^2}(x - 1 + e^{-x}) \quad (4)$$

where x is $(QR_g)^2$, c_p is the stoichiometric polymer concentration (g cm^{-3}), x_p is the fraction of unbound polymer, M_w is the

TABLE 2: Fitting Parameters from Analysis of SANS Data in D_2O at 25 °C

	PEO200		PEO400		PEO900		PEO1500		PPO425		PPO725		PPO1200
laponite RD (wt %)	0.5	1.0	0.5	1.0	0.5	1.0	0.5	1.0	0.5	1.0	0.5	1.0	0.5
σ_R	0.33	0.20	0.31	0.33	0.33	0.33	0.30	0.07	0.31	0.30	0.25	0.06	0.29
ΔR (nm)	0.50	0.78	0.90	0.73	1.06	0.99	1.2	0.87	0.97	0.95	0.91	0.77	1.1
$\phi_{p,shell}$	0.22	0.11	0.22	0.24	0.24	0.24	0.24	0.37	0.29	0.27	0.39	0.49	0.38
x_p	0.96	0.92	0.92	0.84	0.90	0.78	0.88	0.70	0.89	0.78	0.86	0.70	0.43
	1.0[a]	1.0[a]	1.0[a]	1.0[a]	1.0[a]	1.0[a]	0.93[a]	0.87[a]	0.94[a]	0.89[a]	0.89[a]	0.80[a]	0.24[a]
τ			0.10	0.22	0.12	0.22			0.13	0.19			

[a] Calculated from data in ref 14.

polymer molecular weight, N_{Av} is the Avogadro constant, and d_p is the density of the polymer (1.193 and 1.099 g cm^{-3} for PEO and PPO, respectively), whereas ρ_p is the scattering length density of polymer (6.75×10^9 and 3.77×10^9 cm^{-2} for PEO and PPO, respectively).

R_g is the polymer gyration radius evaluated as[28]

$$R_g = \sqrt{\frac{C_\infty N l^2}{6}} \quad (5)$$

where l is the monomer length (3.6 Å) and C_∞ is the characteristic ratio in the limit of long chains (4.0).

Finally, the scattering intensity was fitted by means of the following equation

$$I(Q) = I(Q)_{disk} + I(Q)_{chain} + I_{inc} \quad (6)$$

I_{inc} being the incoherent scattering intensity. Note that the number of fitting parameters is very low (ρ_{shell}, ΔR and σ_R), as we kept the parameters for the laponite RD (R, h, ΔR, ρ_{RD}, $\rho_{solvent}$) fixed by the values obtained from fitting the pure laponite RD system. From ρ_{shell} the relative fraction of polymer in the shell $\phi_{p,shell}$) was calculated as

$$\phi_{p,shell} = (\rho_{shell} - \rho_{solvent})/(\rho_p - \rho_{solvent}) \quad (7)$$

From ρ_{shell} and the shell volume (V_{shell}) we could also determine the fraction of unbound polymer as

$$x_p = 1 - \frac{\rho_{shell} - \rho_{solvent}}{\rho_p - \rho_{solvent}} \frac{^1N_{disk} V_{shell} d_p}{c_p} \quad (8)$$

here the symbols have the same meanings as above.

It is interesting that x_p evaluated independently from the scattering intensity and from the thermodynamic data[14] (see Supporting Information) are in a good agreement (Table 2).

Gelation Time. The gelation time of the laponite RD suspensions in the presence of various polymers was determined. To this aim, two methods were used: (1) the first one was based on viscosity measurements carried out by using a Bohlin Visco 88 rotation viscosimeter at a shear rate of 1007 s^{-1} and (2) the second one used tubes with an internal diameter of 10 mm, each of them containing ca. 1 g of the suspension; the time at which the change from a flowing to an immobile system occurred was determined by inverting the tube at time intervals which were chosen based on the information provided by viscosity.

Usually, the laponite RD concentration was 3 wt % and the polymer concentration was 2.2 wt %. Due to the low solubility of PPO in water, only a few oligomers of low M_w were studied. The temperature was kept at 22.0 ± 0.1 °C.

Results

SANS Studies. As Figure 1 shows, the $I(Q)$ vs Q trend for laponite RD 0.5% in D_2O with or without added polymer are sigmoidal, continuously decreasing curves; very similar to that reported by Cosgrove et al.[11] As a general feature (Figures 1−3), the addition of PEO or PPO induces an increase of the scattered intensity but in most cases does not influence the shape of the curves, which generally level off toward a constant value in the experimental Q-range except for PEO400, PEO900, and PPO425, which exhibit a much stronger increase at low Q. The intensity increases with M_w of the polymer. This effect may reveal the oligomer adsorption at the laponite RD/liquid interface already evidenced by thermodynamic[14] and dynamic light scattering[12] studies. The increase of laponite RD concentration leads to a general increase of the scattered intensity but does not alter the profile of the $I(Q)$ vs Q curve (Figures 2−4).

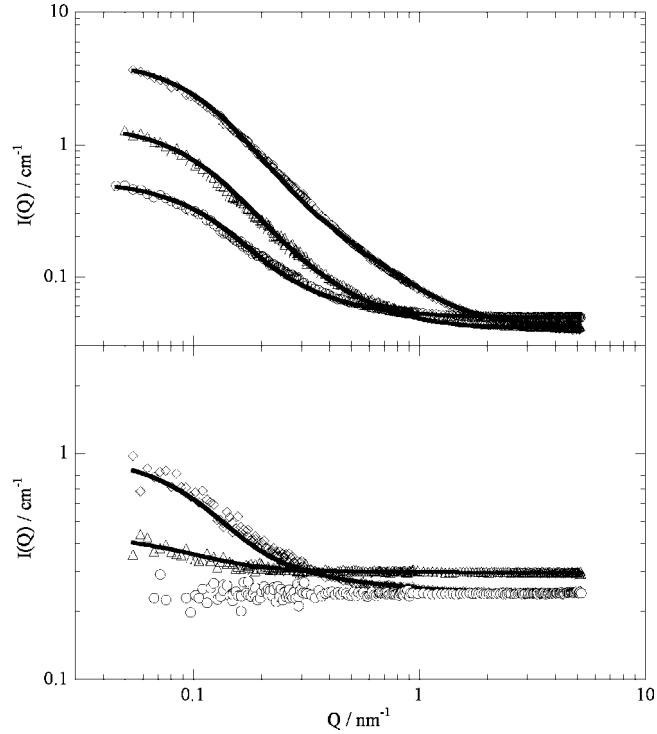

Figure 1. Scattering function of dispersions of laponite RD (0.5 wt %) in the absence (○) and the presence of PEO200 (Δ) and PEO1500 (◇) 1.0 wt % at 25 °C. The solvents are D_2O (top) and D_2O + H_2O (bottom). Lines are best fits according to eq 6.

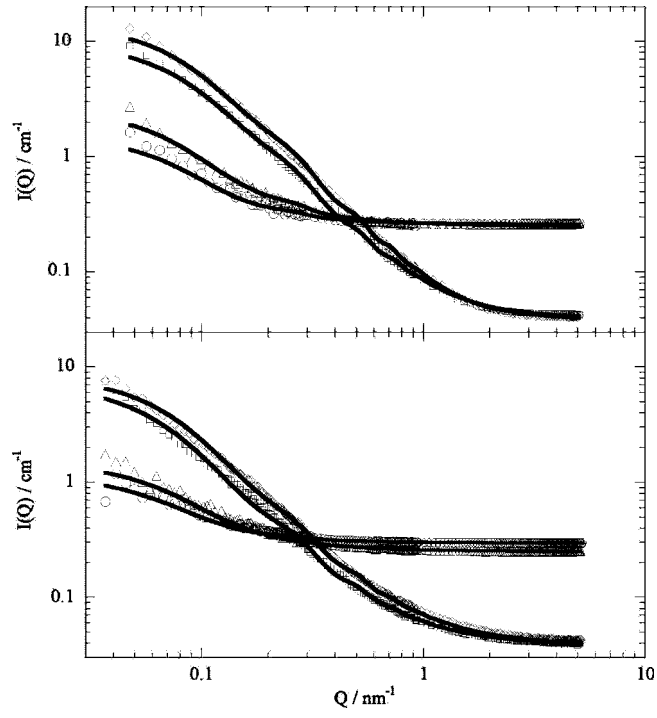

Figure 2. Scattering function of dispersions of laponite RD 1 wt % (top) and 0.5 wt % (bottom) in PEO400 + D_2O (□), PEO400 + D_2O/H_2O (○), PEO900 + D_2O (◇) and PEO900 + D_2O/H_2O (Δ) at 25 °C. The polymer concentration is 1.0 wt %. Lines are best fits according to eq 6 and considering the structure factor for sticky hard spheres.

It has to be noted that for both laponite RD concentrations and for the addition of PEO400, PEO900 and PPO425, $I(Q)$ does not reach a plateau value at low Q. This experimental evidence may be ascribed to (1) the formation of very large

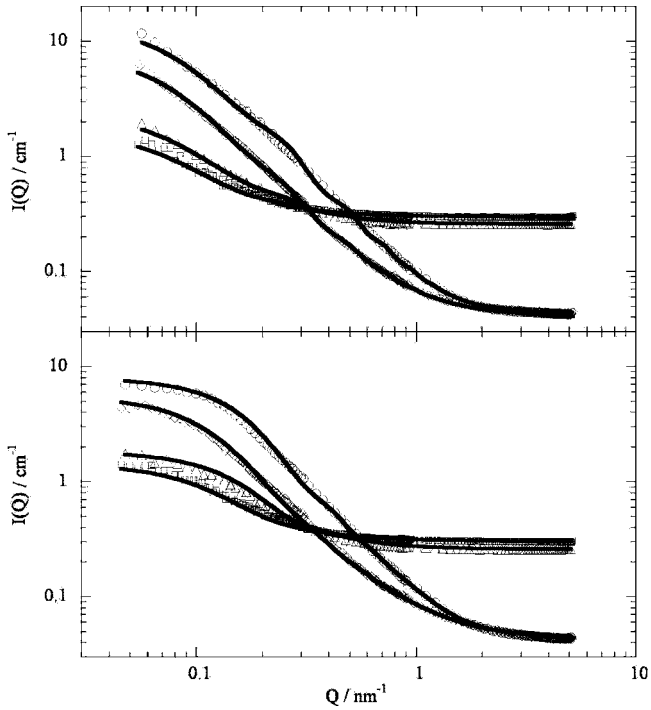

Figure 3. Scattering function of dispersions of laponite RD in the presence of PPO425 (top) and PPO725 (bottom) 1 wt %. Laponite RD concentration is 1 wt % (○, Δ) and 0.5 wt % (◇, □). The solvents are D_2O (○, ◇) and D_2O + H_2O (Δ, □). Lines are best fits according to eq 6 and considering the structure factor for sticky hard spheres in the case of PPO425.

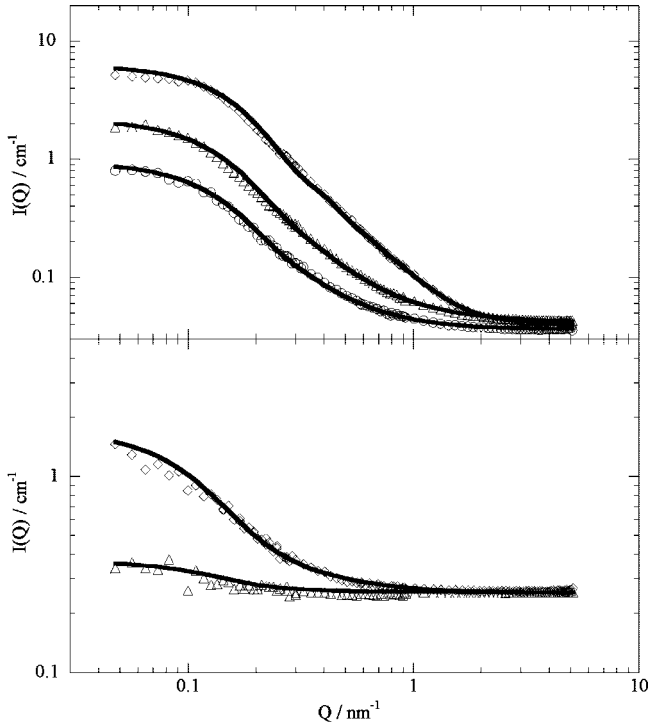

Figure 4. Scattering function of dispersions of laponite RD (1 wt %) in the absence (○) and the presence of PEO200 (Δ) and PEO1500 (◇) 1.0 wt % at 25 °C. The solvents are D_2O (top) and D_2O + H_2O (bottom). Lines are best fits according to eq 6.

clusters or (2) the presence of attractive interactions between the particles.

SANS experiments on the laponite RD suspension (0.5% w/w) in the presence of L35 and 10R5, both having the same

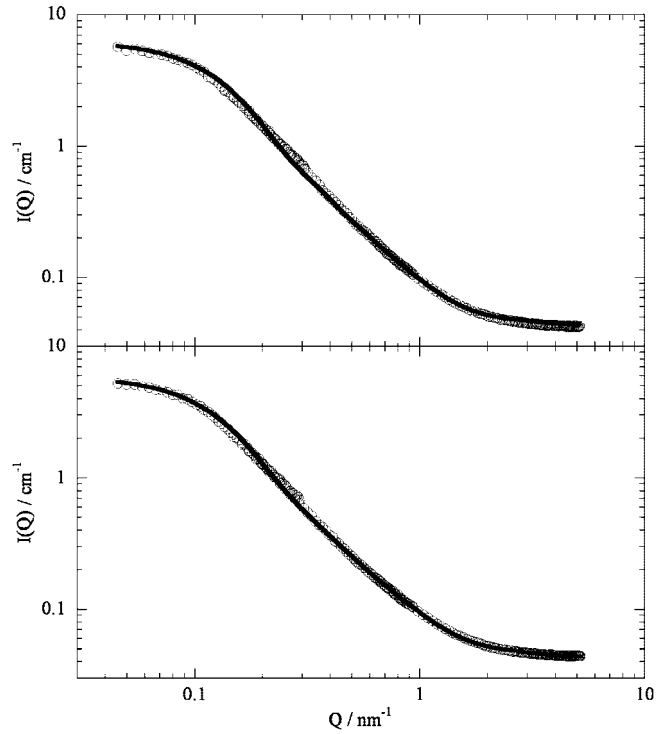

Figure 5. Scattering function of dispersions of laponite RD (0.5 wt %) in L35 (1 wt %, top) and 10R5 (1.0 wt %, bottom) at 25 °C. Lines are best fits according to eq 6.

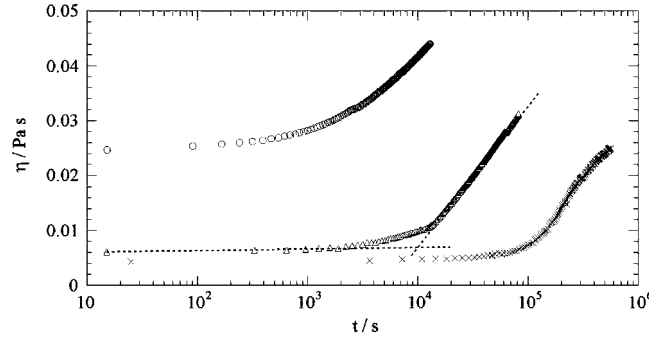

Figure 6. Viscosity at a shear rate of 1007 s^{-1} as a function of time for the laponite RD dispersion in water: (×) 2 wt %; (Δ) 3 wt % and (○) 4 wt %. Broken lines: evaluation of gelation time.

chemical composition but opposite architecture, were also carried out. The $I(Q)$ vs Q curves (Figure 5) are very similar and show the same profiles as those in the presence of the homopolymers that level off at low Q; also, the $I(Q)$ values are independent of the copolymer architecture so that one expects same structural features in agreement with the identical thermodynamics[14] of adsorption on laponite RD observed for both L35 and 10R5.

Gelation Time of Laponite RD Dispersion in the Presence of the Polymers. ***(1) Effect of PEO and PPO Homopolymers.*** The curves of the viscosity (η) as a function of time for the laponite RD dispersion in water were determined for various concentrations (Figure 6). For a given system, η does not change with time up to a critical value thereafter it strongly increases due to the gel formation. The gelation time of the viscosity measurements ($\tau_{g,v}$) was evaluated as the intersection point of two straight lines drawn through the η vs time curve (Figure 6). The more concentrated the mixture the shorter the time required for gelation. On this basis, a laponite RD concentration of 3 wt % was selected for studies in the presence of polymers

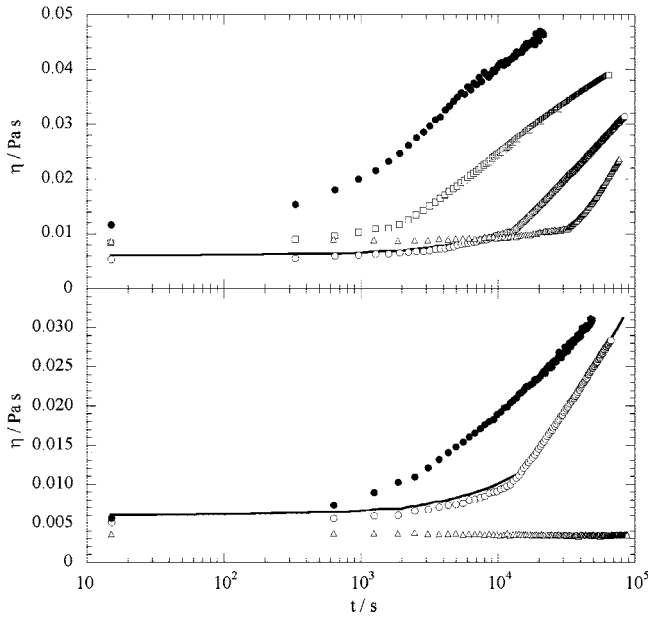

Figure 7. Viscosity at a shear rate of 1007 s^{-1} at 22 °C as a function of time for the laponite RD dispersion 3 wt % in water (black line) and in water + polymer 2.2 wt % mixtures. Top: (○) 1,2-ethanediol; (□) PEO200; (●) PEO400 and (Δ) PEO35000. Bottom: (○) 1,2-propanediol; (●) PPO425; (Δ) PPO725.

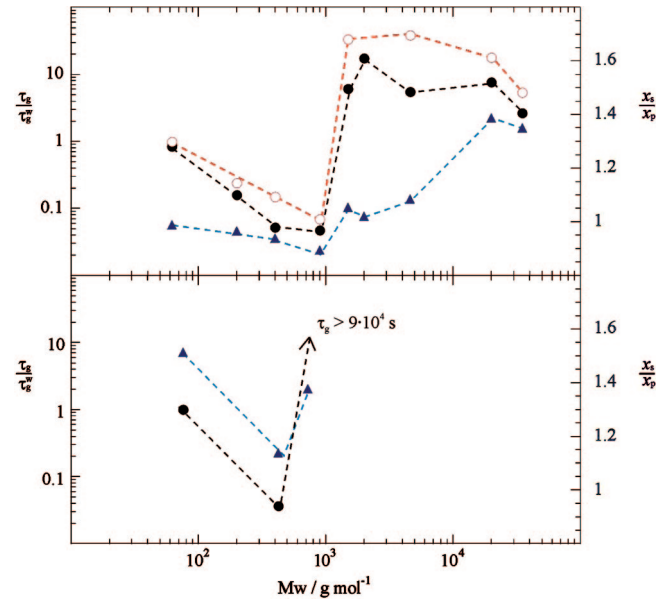

Figure 8. Dependence on the polymer molecular weight of x_s/x_p (▲), gelation time from viscosity $\tau_{g,v}$ (●) and from tube inversion $\tau_{g,t}$ (○) both normalized for the gelation time of laponite Rd 3 wt % in water at 22 °C. Top: poly(ethylene oxides); bottom: poly(propylene oxides). The lines are drawn as a guide to the eye.

because the gelation process can be followed in a convenient time-window.

Representative examples of the curves of η vs time for the laponite RD suspensions (3 wt %) in the presence of PEO and PPO at 2.2 wt % are illustrated in Figure 7. The viscosity values with 2.2 wt % added 1,2-ethanediol and 1,2-propanediol are equal to those in water. Very different effects are observed upon changing the molecular weight of the added polymer. In fact, compared to the trend in water, the increase of the PEO molecular weight to 900 g mol^{-1} shifts the viscosity curves to shorter times whereas the opposite takes place for larger M_w. Amazingly, this is a very intriguing behavior which has not been highlighted previously. Namely, $\tau_{g,v}$ is a decreasing function of M_w up to 900 g mol^{-1} and an increasing function for larger M_w. The trend of $\tau_{g,v}$ vs M_w, plotted in Figure 8, demonstrates the opposite role played by PEO for low and high M_w. A similar effect is observed for PPO except that for larger M_w PPO is not any more soluble in water. It should be noted that the gelation process occurring in our systems may be affected by the shear (of the viscosity measurements) as observed in similar systems in the literature[16,17] reporting reversible shear-induced gelation for the laponite RD/PEO of 3×10^5 g mol^{-1} system. Therefore in our experiments care was taken in order to ensure that identical shear conditions were chosen for the various viscosity measurements. The gelation time values determined from the tube inversion measurements ($\tau_{g,t}$) as functions of M_w describe the same profile as that from viscosity data but are always shifted toward larger values (Figure 8). This is to be expected as it describes the point where during the gelation process a yield stress is reached that is beyond the value exerted by the own weight of the sample and not just the onset of the viscosity increase.

(2) Effect of Triblock Copolymers Based on PEO and PPO Blocks. The interesting gelation time dependence for the PEO and PPO oligomers induced us to study in addition aqueous laponite RD suspension in the presence of copolymers based on PEO and PPO blocks. To this aim as copolymers we choose the following:

(1) F68, F88, and F108 having the same EO/PO ratio but different M_w;
(2) L35 and 10R5 having the same M_w and EO/PO ratio but an opposite architecture;
(3) L64 and F68 having an identical hydrophobic PPO block but differing with respect to the length of the PEO block, thereby probing the effect of copolymer hydrophilicity.

As a general result, triblock copolymers are more effective in retarding the laponite RD gelation process compared to the homopolymers so that an additivity of the behavior of the different blocks is not observed. Apparently these amphiphiles exhibit a general stabilizing effect. Furthermore, for the investigated copolymers, a specificity of each macromolecule can be detected. As Figure 9 shows, within the time of investigation, compared to water, the gelation process is retarded by ca. 25 h in the presence of 10R5 and it does not take place at least within 110 h in the presence of L35. As concerns the role of F68, F88, and F108, for at least 148 h the gelation is suppressed (Figure 9). The lengthening of the PEO blocks (F68 instead of L64), having the same PPO segment, retards the gel formation which occurs after 56 h in the presence of L64.

Discussion

Structures of the Laponite RD/Polymer Suspensions. The R_G vs M_w trends for both laponite RD compositions are illustrated in Figure 10; the shape of the graphs is independent of laponite RD amount while the R_G values are smaller for the more concentrated suspension. Presumably they are lower as a consequence of the increased number of particles which produce in general more pronounced repulsive steric forces, which is reflected in the structure factor. A careful inspection of Figure 10 puts into evidence that R_G increases in the region at low M_w whereas the opposite occurs for larger M_w. Such a trend evidence a peculiarity exactly in the region where the τ_g vs M_w curve presents a minimum (Figure 8) suggesting that both parameters are sensitive to the same phenomenon. This behavior can be clearly explained by remembering that R_G is basically given by two contributions:

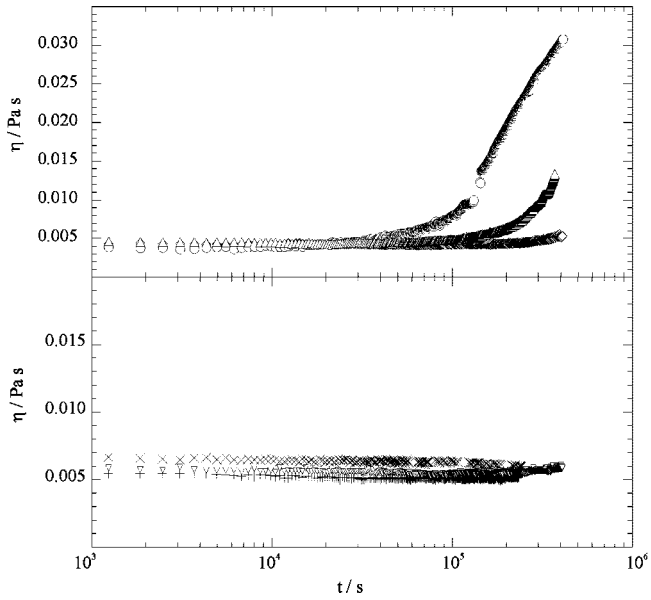

Figure 9. Viscosity as a function of time for the laponite RD dispersion 3 wt % in the water+copolymer 2.2 wt % mixtures. (◇), L35; (○), 10R5; (Δ), L64; (×), F108; (▼), F88; (+), F68.

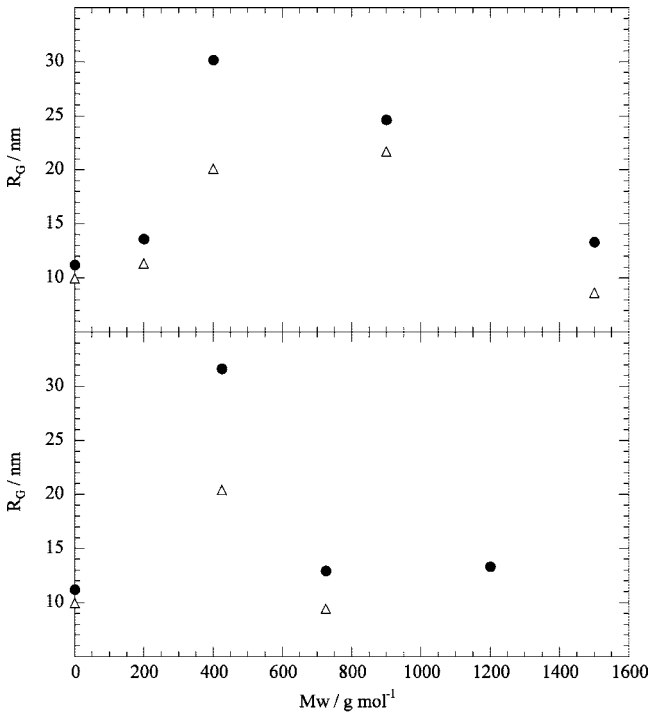

Figure 10. Dependence on the polymer molecular weight of R_G for laponite RD + PEO + D_2O (top) and laponite RD + PPO + D_2O (bottom). The laponite RD concentrations are 1.0 wt % (Δ) and 0.5 wt % (●).

(1) the size of the particles coated with the polymer;
(2) the interactions between the laponite RD particles.

R_G reveals quite strong attractive forces for PEO400, PEO900, and PPO425 while repulsive steric forces are present for larger polymers. The duality of the involved forces may explain the different effect of the polymers toward the gelation velocity; in fact, attractive interactions are consistent with the observed speeding up of gelation.

The $I(Q = 0)$ values exhibit a M_w dependence similar to that of R_G (Figure 11) with a very peculiar behavior at intermediate PEO sizes. $I(Q = 0)$ is given by ${}^1N_{disk}\langle V\rangle^2\Delta\rho^2 S(Q = 0)$ where

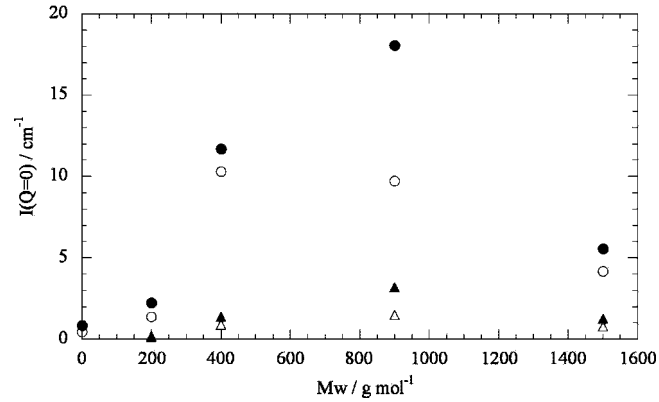

Figure 11. Dependence on the polymer molecular weight of $I(0)$ for laponite RD + PEO + D_2O (circles) and laponite RD + PEO + D_2O + H_2O (triangles). The laponite RD concentrations are 1.0 wt % (filled symbols) and 0.5 wt % (empty symbols).

$\langle V\rangle$ is the average volume of the aggregate, $\Delta\rho$ is the scattering contrast between the particle and the solvent whereas $S(Q = 0)$ is the structure factor at $Q = 0$. If $S(Q = 0)$ is unity, one predicts an increase of $I(Q = 0)$ as a consequence of the V increase; that is experimentally observed only at low M_w. Therefore, one may deduce that $S(Q = 0)$ is a function of M_w; accordingly, $S(Q = 0)$ assumes values larger and smaller than unity when attractive and repulsive interactions take place, respectively. This description fully fits the behavior of our systems described by R_G as well as the gelation time.

The SANS curves in the entire range of Q were fitted by a model of noninteracting core+shell disk with polydisperse radii and taking into account the contribution of the polymer freely dispersed in the solvent (Table 2).

Previous thermodynamic studies[14] reported that the adsorption occurs *via* the attractive interactions between negatively charged laponite RD surface and the −OH groups while the laponite RD positive edge interacts with the ether oxygen. It is noteworthy that the thermodynamic properties of adsorption on laponite RD particles[14] exhibit differences in the low and high M_w regions. This finding was ascribed[14] to the different behavior between the polymer in the adsorbed and the free states strongly dependent on M_w. For instance,[29,30] high M_w polymers have a conformation similar to the crystalline state and form helical structures in water whereas low M_w polymers exhibit a less ordered structure. These features are maintained also when the polymer is adsorbed onto the laponite RD particles.[14] The thickness of the polymer layer increases with M_w (Table 2) and such a variation is consistent with findings reported by Cosgrove et al.[11] for very high M_w. The adsorbed polymer is in a more compact conformation compared to a random coil distribution which would allow for a ΔR value at least one-half larger than the experimental value. The same conclusion can be drawn for both L35 and 10R5 which, in turn, possess the same ΔR values (1 nm). This result is opposite to the finding[31] for the adsorption of L64 on polystyrene nanoparticles for which the experimental ΔR (10 nm) is larger than that calculated according to the random coil configuration (4.4 nm). In this case, the number of sites of interactions is low and the copolymer is extended into the aqueous phase.

The fraction of the polymer in the shell formed around the laponite RD particles is nearly independent of M_w the magnitude of which is similar to that reported[11] for very large PEOs. These values (ca. 0.24) reflect a large amount of water present in the shell which decreases in the presence of the more hydrophobic PPO 725 (0.39).

TABLE 3: Fitting Parameters from Analysis of SANS Data in $D_2O + H_2O$ Mixture at 25 °C

	PEO200		PEO400		PEO900		PEO1500		PPO425		PPO725	
laponite RD (wt %)	0.5	1.0	0.5	1.0	0.5	1.0	0.5	1.0	0.5	1.0	0.5	1.0
σ_R	0.33	0.22	0.32	0.36	0.30	0.35	0.32	0.28	0.31	0.31	0.28	0.10
ΔR (nm)	0.34	0.73	1.1	1.2	1.24	1.08	1.5	0.94	1.29	1.1.94	1.28	1.6
$\phi_{p,shell}$	0.31	0.10	0.19	0.15	0.23	0.21	0.20	0.27	0.22	0.12	0.28	0.21
τ			0.13	0.21	0.13	0.20			0.14	0.24		

By increasing the laponite RD concentration and keeping constant the polymer composition, ΔR slightly changes.

It is noteworthy that all these insights agree with those provided by independent experiments which used as solvent the $D_2O + H_2O$ mixture matching the laponite RD. In fact, the scattering intensity of the mixtures containing D_2O and H_2O were successfully fitted and provided parameters (Table 3) which agree with those obtained fitting data in D_2O solvent (Table 2).

Equation 6 was not able to fit the scattering curves which do not reach a plateau value in the low Q regime, namely PEO400/laponite RD, PEO900/laponite RD, and PPO425/laponite RD. In these cases, the structure factor for sticky hard spheres,[32] which takes into account attractive interparticle interactions, was calculated. The origin of the attraction is attributed to the depletion effect which describes the expulsion of the polymer from the gap, generated when the particles approach to a distance shorter than the polymer diameter, producing osmotic pressure differences that favor the particles attraction. It is noteworthy that in the SANS data fitting procedure such a model introduces only one additional parameter, namely, the stickiness parameter (τ) which decreases with increasing attractive forces. A careful inspection of data in Table 2 shows that, for a given laponite RD composition, τ is nearly independent of the polymer nature. By increasing the laponite RD content, the τ value increases according to the larger repulsive forces exercising between the particles.

Finally, as concerns L35 and 10R5, they form a monolayer adsorbed on the laponite RD particles with a thickness of 1.0 nm which is much smaller than that of the random coil model (3.7 nm). The shell adsorbed on the laponite RD particles is more hydrated than the corresponding oligomers being basically formed by ca. 50% of water, which is slightly larger in the shell composed of L35.

Formation of Gels in the Presence of PEO and PPO Polymers. Several papers[33–38] have been devoted to the laponite RD gelation in the absence and the presence of polymers the mechanism of which is still object of controversy.[18] The gel formation in water was ascribed to the build-up of fractal clusters,[33,37–40] to a card-house structure[40–45] and to the colloidal glass.[34]

The behavior observed by us is not only very intriguing but also strikingly different from what has been published so far. The binding to the clay particles is much more pronounced for PEO or PPO of intermediate size and directly correlated to the rheological behavior of the corresponding clay/polymer systems. We now propose plausible explanations for the peculiar behavior of the oligomers of PEO and PPO on the laponite RD gelation.

Figure 8 shows the M_w dependence of τ_g and x_s/x_p, e.g., the ratio between the fraction of laponite RD sites occupied by the polymer (x_s) and the fraction of the polymer dispersed in the aqueous phase (x_p). Both depend in a similar fashion on the polymer M_w. For PEO Figure 8 shows two distinct regions: the first where τ_g decreases with M_w up to 900 g mol^{-1} and the second one where the opposite occurs. It has been reported[18] that the polymer strongly slowed the gelation process and the effect is more pronounced for larger M_w (being comprised between 13×10^3 and 1.07×10^6 g mol^{-1}). This phenomenon was attributed to the polymer acting[18] to either reduce the particles interactions due to the steric barrier or the effective volume fraction. It was also stated[16,17] that when the laponite RD surface is not fully covered, the polymer bridges some disks and generates gels. Once the polymer saturates the laponite RD particles, stable sols are formed.[20] We can verify through quantitative computations whether this model fits our results. By defining one laponite RD site as the portion of particle interacting with one polymer molecule,[14] x_s is calculated from the equilibrium constants for the polymer adsorption.[14] The plot of x_s against M_w interestingly illustrates (Figure 12) that PEO35000 occupies all of the laponite RD sites ($x_s \approx 1$); nevertheless, a gel is formed. The smallest adsorbing polymer (PEO200) covers almost of the laponite RD sites available ($x_s = 0.97$) and the fully extended molecule of ca. 2 nm[46] cannot bridge laponite RD disks because of its short chain. Nevertheless, PEO200 not only induces gelation but it accelerates this process substantially which occurs now within a time 29 min ($\tau_{g,v}$) compared to 167 min for pure water. Therefore, in spite of the fact that the oligomers cover almost all of the adsorption sites ($0.97 \leq x_s \leq 0.8$), they form gels rapidly, even though the steric barrier effect is present (likely small due to the relatively small polymeric chain entropy) and their size is too small to prevent a bridging of the laponite RD particles. The interactions between charged laponite RD particles are not affected by the solvent dielectric constant which varies very slightly with M_w.[47] Another potential effect is related to the depletion force via the osmotic effect. Morvan et al.[48] reported that polyelectrolytes dispersed in the water phase induce a depletion effect with the consequence of a phase transition of clay platelets. Such a phenomenon is present for nonadsorbing polymer. However, even though in our case the polymers are adsorbed on laponite RD surface, the amount dispersed in the aqueous phase may generate a depletion effect. The attractive depletion potential is different from zero when the distance between the surfaces of two laponite RD particles is equal or less to the polymer diameter.[49] By using a simple primitive cubic cell model and considering laponite RD as a rotating disk, a mean spacing of 2 nm between laponite RD surfaces is obtained for a laponite RD concentration of 3 wt %. This value, comparable to the oligomers diameter (calculated by means of eq 5) shows that depletion is a possible mechanism in our systems. Furthermore, it is interesting that x_p is nearly unity to $M_w = 900$ g mol^{-1}, after which it decreases with M_w (Figure 12). These findings are consistent with the previous SANS results on the laponite RD dispersion in the presence of polymers with intermediate M_w which presented stickiness parameters.

The phase behavior of laponite RD affected by depletion can be expressed by the depletion potential. Van der Kooij et al.[50] reported the maximum depth of the depletion potential (W_d) for parallel plates

$$W_d/k_BT = -(3/2)\phi_{p,free}\left(\frac{\Delta R + R}{R_g}\right)^2 \quad (9)$$

where k_B is the Boltzmann constant, $\phi_{p,free}$ is the volume fraction of unbound polymer while the other symbols assume the same meaning as above. The W_d values were calculated by introducing in eq 9 the values of ΔR (Table 2) and R (12.7 nm) previously determined from SANS experiments, R_g calculated by means of eq 5 and $\phi_{p,free}$ computed according to the procedure described in the Supporting Information. W_d depends on M_w (Figure 13) as it sharply changes for $M_w < 10^3$ and slightly does for higher M_w. It is striking that the W_d critical value for the gelation of laponite RD is close to the depletion potential ($-3k_BT$) usually required for the depletion-induced phase transition of hard spheres. Therefore, it appears that only PEO with $M_w < 10^3$ g mol^{-1} enhances the phase transition like gel-formation due to the depletion effect corroborating the previous arguments. In conclusion, inspecting x_p and x_s one deduces that both the polymer adsorption (which sterically stabilizes the laponite RD particles) and the depletion (which favors gelation) can clearly describe our data. Accordingly, the x_s/x_p ratio vs M_w trends (Figure 8) exhibit peculiarities at $M_w = 900$ and 425 g mol^{-1} for PEO and PPO, respectively. What is interesting is that for both polymers the profile of these curves is identical to that of the τ_g vs M_w suggesting that the gelation rate is correlated to the phenomena controlling the polymer adsorption. When the balance between the steric forces and the depletion attractive forces undergoes an abrupt change the gelation time also undergoes a sharp variation. These arguments explain the negligible influence of very small molecules such as 1,2-ethanediol and 1,2-propanediol. Our interpretation of the depletion effect differs from the Baghdadi et al.[21] idea that the melting of laponite RD glass generated by PEO of variable M_w (from 13×10^3 to 60×10^3 g mol^{-1}) is ascribable to a depletion attraction which reduces the effective volume fraction and allows flowing.

Another way to look at this phenomenon from a kinetic point of view would be the effectiveness of the attached PEO in stabilizing the laponite RD particles. The PEO covering should reduce the electrostatic repulsion between the laponite RD particles as the PEO dipoles interact with the particles charged sites by effectively shielding them. Accordingly, a larger probability for the covered laponite RD particle to collide and agglomerate with each other is expected. For the small PEO, this may explain an enhanced tendency for gelation as the steric repulsion is low and being small molecules their dynamics and ability to be replaced on the particles binding sites is fast, as the shorter polymers constitute a more flexible state of the covering polymer. The segments of the larger PEO protrude into the surrounding solution and, correspondingly, the particles steric repulsion will increase thereby effectively hindering the particles to get into direct contact as necessary for gelation to occur. Also, the dynamic mobility of larger PEO is less, leading to a further hindrance in having two laponite RD platelets in direct contact. The case of PPO is even more striking as PPO 425 generates a substantial increase of the gelation rate while the larger PPO 725 suppresses the gelation completely, as even after 6 months no gelation for that sample is observed. Here the gelation behavior appears even more affected by the precise length of the water-soluble polymer. This can be ascribed to the stronger PPO binding to the clay particles compared to PEO.[14] Accordingly, for a comparable increase in polymer size, the equilibrium constant of adsorption of PPO on laponite RD is ca. 5 times larger than that of PEO.[14] This difference is basically ascribed to the inductive effect of the methyl group on the ether oxygen which is attracted by the positively charged edges of the laponite RD disks.

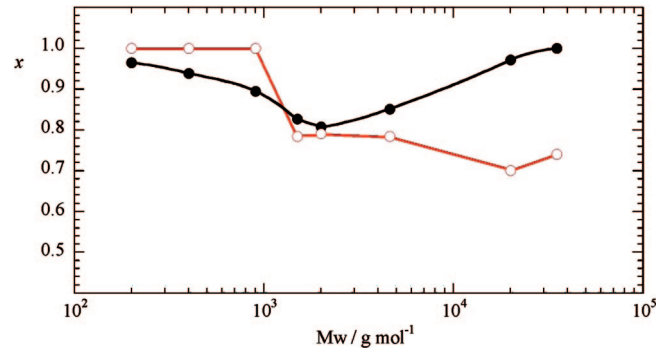

Figure 12. Fractions of laponite RD sites occupied by the polymer x_s (●) and of freely dispersed polymer x_p (○) as functions of the polymer molecular weight. The lines are drawn as a guide to the eye.

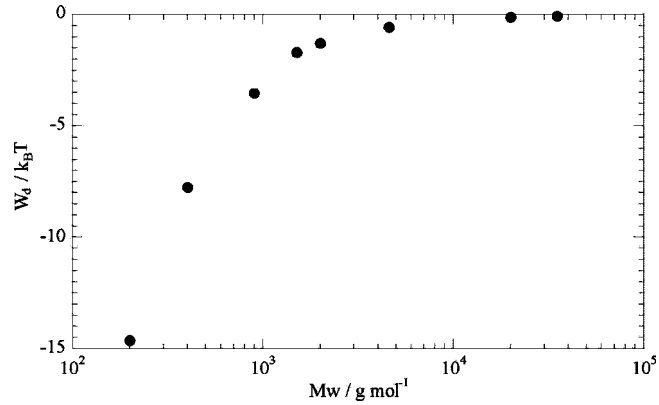

Figure 13. Maximum depth of the depletion potential as a function of the PEO molecular weight.

Conclusions

The structure of the aqueous laponite RD/polymer suspensions was investigated by means of SANS studies for the case of PEO and PPO oligomers as well as copolymers based on PEO and PPO blocks. The apparent radius of gyration of the mixed aggregates increases in the region at low M_w whereas it decreases for larger M_w. This behavior is ascribed to: (1) the size of the particles coated with the polymer and (2) the forces between the laponite RD particles which are attractive for small polymers and repulsive for large polymers. The M_w influences the thickness of the adsorbed polymer which is in all cases a more compact conformation compared to a random coil distribution; on the contrary, the fraction of the polymer in the shell formed around the laponite RD particles is nearly independent of M_w. The SANS data show a pronounced attractive interaction between the clay/polymer systems for PEO or PPO of intermediate chain length. Whenever such a pronounced attractive interaction is observed for the 0.5 and 1 wt % laponite RD concentrations a much enhanced gelation speed is observed at higher clay concentration, i.e. the microstructure of the clay particles is directly correlated to the observed macroscopic gelation behavior.

Accordingly the addition of PEO and PPO to laponite RD clay has a striking and complex effect on the gelation properties of laponite RD particles, exhibiting a pronounced maximum of the gelation rate at intermediate molecular weight of PEO or PPO. For the low molecular weight case of PEO and PPO one observes a speeding up of the gelation by more than a factor of

10. However, very abruptly for M_w larger than 1000 g mol^{-1} of PEO and 600 g mol^{-1} of PPO this effect is reversed and the gelation kinetics is slowed down by more than a factor of 100 for the case of PEO. For still higher PEO molecular weights the gelation kinetics remains slowed down and this is even more pronounced for PPO as here the gelation becomes completely suppressed already for the highest chosen molecular weight of 725 g mol^{-1}. Apparently subtle changes in the structure of the added polymer have a pronounced impact on the structure and interaction of the formed mixed aggregates which translate into a largely different macroscopic behavior of these systems.

A clear correlation exists between the structure of the polymer covered clay particles and their gelation behavior. The more intense the attractive interaction between the polymer covered laponite particles the faster the gelation speed where the interparticle attraction arises from depletion interactions due to still unbound polymer. From these insights one may deduce that these kinds of gels can be finely modulated by changing either the laponite RD and polymer compositions or the polymer size and nature to obtain properties for specific purposes like, for example, the application in the Cultural Heritage topic.

Acknowledgment. The work was financially supported by Vigoni and CORI projects 2005 and by MiUR (PRIN 2006, "Design of functional nanostructured systems for the restoration and the conservation of cultural heritage", prot. 2006088875_002). G.L. is grateful to the Università degli Studi di Palermo for the "Assegno di Ricerca" Fellowship. The experiments at BENSC in Berlin were supported by the European Commission under the 6th Framework Programme through the Key Action: Strengthening the European Research Area, Research Infrastructures, Contract No. RII3-CT-2003-505925 (NMI3).

Supporting Information Available: Text discussing calculation of the free polymer fraction. This material is available free of charge via the Internet at http://pubs.acs.org.

References and Notes

(1) Fraile, J. M.; Garcýa, J. I.; Harmer, M. A.; Herreryas, C. I.; Mayoral, J. A.; Reiser, O.; Werner, H. *J. Mater. Chem.* **2002**, *12*, 3290.
(2) Barhoumi, M.; Beurroies, I.; Denoyel, R.; Saïd, H.; Hanna, K. *Colloids Surf. A: Physicochem. Eng. Asp.* **2003**, *223*, 63.
(3) Gherardi, B.; Tahani, A.; Levitz, P.; Bergaya, F. *Appl. Clay Sci.* **1996**, *11*, 163.
(4) Yamaguchi, Y.; Hoffmann, H. *Colloids Surf. A: Physicochem. Eng. Asp.* **1997**, *121*, 67.
(5) Rosta, L.; von Gunten, H. R. *J. Colloid Interface Sci.* **1990**, *134*, 397.
(6) Pignon, F.; Magnin, A.; Piau, J. M. *Phys. Rev. Lett.* **1997**, *79*, 4689.
(7) Willenbacher, N. *J. Colloid Interface Sci.* **1996**, *182*, 501.
(8) Giannelis, E. P.; Krishnamoorti, R.; Manias, E. *Adv. Polym. Sci.* **1999**, *138*, 108.
(9) Wendy, L.; Jannasch, P.; Maurer, F. H. J. *Polymer* **2005**, *46*, 915.
(10) De Lisi, R.; Lazzara, G.; Milioto, S.; Muratore, N. *J. Therm. Anal. Calorim.* **2007**, *87*, 61.
(11) Nelson, A.; Cosgrove, T. *Langmuir* **2004**, *20*, 2298.
(12) Nelson, A.; Cosgrove, T. *Langmuir* **2004**, *20*, 10382.
(13) Mongonfry, P.; Nicolai, T.; Tassin, J. F. *J. Colloid Interface Sci.* **2004**, *275*, 191.
(14) De Lisi, R.; Lazzara, G.; Lombardo, R.; Milioto, S.; Muratore, N.; Turco Liveri, M. L. *Phys. Chem. Chem. Phys.* **2005**, *7*, 3994.
(15) Vanderbeek, G. P.; Cohen-Stuart, M. A. *J. Phys. IV* **1988**, *49*, 1449.
(16) Zebrowski, J.; Prasad, V.; Zhang, W.; Walker, L. M.; Weitz, D. A. *Colloids Surf. A: Physicochem. Eng. Asp.* **2004**, *240*, 187.
(17) Pozzo, D. G.; Walker, L. M. *Colloids Surf. A: Physicochem. Eng. Asp.* **2003**, *213*, 189.
(18) Baghdadi, H. A.; Sardinha, H.; Bhatia, S. R. *J. Polym. Sci., Part B: Polym. Phys.* **2005**, *43*, 233.
(19) Martin, C.; Pignon, F.; Piau, J. M.; Magnin, A.; Lindner, P.; Cabane, B. *Phys. Rev. E* **2002**, *21*, 401.
(20) Lal, J.; Auvray, L. *J. Appl. Crystallogr.* **2000**, *33*, 673.
(21) Baghdadi, H. A.; Jensen, E. C.; Easwar, N.; Bhatia, S. R. *Rheol. Acta* **2008**, *47*, 121.
(22) Keiderling, U.; Wiedenmann, A. *Physica B* **1995**, *213 & 214*, 895.
(23) Chen, S. H.; Lin, T. L. *Methods Exp. Phys.* **1987**, *23B*, 489.
(24) Keiderling, U. *Physica B* **1997**, *234*−*236*, 1111.
(25) Keiderling, U. *Appl. Phys. A: Mater. Sci. Process.* **2002**, *74*, S1455.
(26) Yu, V.; Cser, L.; Grósz, T.; Jancsó, G.; Ostanevich, Yu. M. *J. Phys. Chem.* **1992**, *96*, 976.
(27) Debye, P. *J. Phys. Colloid Chem.* **1947**, *51*, 18.
(28) Flory, P. J. *Statistical Mechanics of Chain Molecules*; Interscience: New York, 1969.
(29) Kjellander, R.; Florin, E. *J. Chem. Soc., Faraday Trans.* **1981**, *77*, 2053.
(30) Graham, N. B.; Zulfiquar, M.; Nwachuku, N. E.; Rashid, A. *Polymer* **1989**, *30*, 528.
(31) De Lisi, R.; Lazzara, G.; Milioto, S.; Muratore, N. *Phys. Chem. Chem. Phys.* **2008**, *10*, 794.
(32) Baxter, R. J. *J. Chem. Phys.* **1968**, *49*, 2770.
(33) Nicolai, T.; Cocard, S. *Eur. Phys. J. E* **2001**, *5*, 221.
(34) Bonn, D.; Kellay, H.; Tanaka, H.; Wegdam, G.; Meunier, J. *Langmuir* **1999**, *15*, 7534.
(35) Saunders, J. M.; Goodwin, J. W.; Richardson, R. M.; Vincent, B. *J. Phys. Chem. B* **1999**, *103*, 9211.
(36) Gabriel, J. C. P.; Sanchez, C.; Davidson, P. *J. Phys. Chem.* **1996**, *100*, 11139.
(37) Mourchid, A.; Lecolier, E.; Van Damme, H.; Levitz, P. *Langmuir* **1998**, *14*, 4718.
(38) Tanaka, H.; Jabbari-Farouji, S.; Meunier, J.; Bonn, D. *Phys. Rev. E* **2005**, *71*, 021402.
(39) Pignon, F.; Piau, J. M.; Magnin, A. *Phys. Rev. Lett.* **1996**, *76*, 4857.
(40) Pignon, F.; Magnin, A.; Piau, J. M.; Cabane, B.; Lindner, P.; Diat, O. *Phys. Rev. E* **1997**, *56*, 3281.
(41) Garfinkelshweky, D.; Yariv, S. *Colloid Polym. Sci.* **1995**, *273*, 453.
(42) Permien, T.; Lagaly, G. *Colloid Polym. Sci.* **1994**, *272*, 1306.
(43) Axford, S. D. T.; Herrington, T. M. *J. Chem. Soc. Faraday Trans.* **1994**, *90*, 2085.
(44) Lockhart, N. C. *J. Colloid Interface Sci.* **1980**, *74*, 509.
(45) Morvan, M.; Espinat, D.; Lambard, J.; Zemb, T. *Colloids Surf. A* **1994**, *82*, 193.
(46) Lazzara, G.; Milioto, S.; Gradzielski, M. *Phys. Chem. Chem. Phys.* **2006**, *8*, 2299.
(47) Capuano, F.; Vergara, A.; Paduano, L.; Annunziata, O.; Sartorio, R. *J. Phys. Chem. B* **2003**, *107*, 12363.
(48) Morvan, M.; Espinat, D.; Vascon, R.; Lambard, J.; Zemb, T. *Langmuir* **1994**, *10*, 2569.
(49) Asakura, S.; Oosawa, F. *J. Polym. Sci.* **1958**, *33*, 183.
(50) van der Kooij, F. M.; Vogel, M.; Lekkerkerker, H. N. W. *Phys. Rev. E* **2000**, *62*, 5397.

JP8024073